**Journal of Fisheries**
Volume 14 Issue 1 April 2026
Peer Reviewed | Open Access

eISSN 2311-3111
pISSN 2311-729X

DOI: https://doi.org/10.17017/j.fish.1165

**Original Article**

# Antimicrobial resistance and phage sensitivity of *Chryseobacterium* sp. isolated from diseased rainbow trout (*Oncorhynchus mykiss*)

**Mustafa Ustundag**[1] • **Berrin Ustundag**[2]

[1] *Department of Chemistry and Chemical Management Technologies, Muradiye Vocational School, Van Yuzuncu Yıl University, Van 65080, Türkiye*
[2] *Department of Scientific Research Project Office, Van Yuzuncu Yıl University, Van 65080, Türkiye*

**Correspondence**
Mustafa Ustundag; Department of Chemistry and Chemical Management Technologies, Muradiye Vocational School, Van Yuzuncu Yıl University, Van 65080, Türkiye
mustafaustundag@yyu.edu.tr

**Manuscript history**
Received 1 December 2025 | Accepted 19 December 2025 | Published online 23 December 2025

**Citation**
Ustundag M, Ustundag B (2026) Antimicrobial resistance and phage sensitivity of *Chryseobacterium* sp. isolated from diseased rainbow trout (*Oncorhynchus mykiss*). Journal of Fisheries 14(1): 141207. DOI: 10.17017/j.fish.1165

**Abstract**
This study aimed to isolate and characterize bacteriophages infecting *Chryseobacterium* sp., an opportunistic pathogen responsible for considerable mortality in rainbow trout (*Oncorhynchus mykiss* Walbaum, 1792) aquaculture. *Chryseobacterium* isolates were recovered from diseased trout collected from aquaculture facilities in Mersin and Van (Türkiye) using Anacker–Ordal medium. Identification was performed through API 20E/20ZYM biochemical profiling and 16S rRNA gene sequencing. Antibiotic susceptibility was evaluated by the Kirby–Bauer disk diffusion method following CLSI and EUCAST guidelines. Phages were isolated from water samples via 0.22 µm filtration and purified using the double-layer agar method. Antimicrobial susceptibility testing revealed that *Chryseobacterium* isolates were sensitive to enrofloxacin, oxolinic acid, and ciprofloxacin, but exhibited pronounced resistance to most β-lactam and aminoglycoside antibiotics. A total of 19 lytic phages (CV1 – CV19) were successfully isolated. They displayed latent periods between 2.5 and 7.5 h and burst sizes ranging from 20 to 235 PFU per cell. The highest burst size and shortest latent period were recorded for the CV5 phage. Adsorption rate constants showed phage-specific variability, with overall values ranging from $1.05\times10^{-6}$ to $2.55\times10^{-6}$ mL·min$^{-1}$. Genome sizes were estimated at 48 – 75 kb. TEM revealed typical tailed morphologies consistent with the order *Caudovirales*. Host range assays showed strong species specificity, with limited cross-activity against *Flavobacterium psychrophilum* and *Enterococcus faecalis*. The findings confirm that these phages possess traits favorable for use as eco-friendly biocontrol agents, offering a promising strategy to mitigate *Chryseobacterium*-associated infections and reduce antibiotic dependence in trout hatcheries.

**Keywords:** aquaculture; bacteriophage; *Chryseobacterium*; phage therapy

## 1 | INTRODUCTION

Aquaculture is a rapidly expanding food sector worldwide and meets a substantial share of the global population's protein demand. Aquaculture is continually challenged by environmental stressors and the presence of pathogenic microorganisms that are part of the aquatic ecosystem (Stephen *et al*. 2023). In particular, during sensitive developmental stages when the fish immune system is weakened, pathogenic bacteria can adversely affect fish health (Wang *et al*. 2020). This situation both causes mortalities in aquaculture, leading to economic losses, and threatens the sustainability of the sector (Rosado *et al*.

2019). Bacterial diseases in aquaculture increase production costs, reduce product quality, and in some cases lead to mass fish mortalities. Therefore, effective control of bacterial infections in aquaculture is critical for the sustainability of the industry (De Schryver *et al*. 2012). In this context, alongside many aquatic pathogenic bacteria, species of *Chryseobacterium* are among the important bacterial pathogens associated with diseases in commercially valuable trout (e.g. *Salmo trutta* and *Oncorhynchus mykiss*) (Loch and Faisal 2014). The genus *Chryseobacterium* comprises gram-negative, aerobic, rod-shaped bacteria. While these bacteria are commonly found in aquatic ecosystems, their opportunistic pathogenicity can lead to various infections in fish species and cause mortalities (Huang 2025). Indeed, studies have reported that *Chryseobacterium piscicola* has caused deaths in Atlantic salmon (*Salmo salar*) and rainbow trout (*O. mykiss*) farmed in Chile and Finland, and that *Chryseobacterium chaponense* has likewise caused mortalities in Atlantic salmon reared in Chile (Kämpfer *et al*. 2015; Saticioglu *et al*. 2019). In a study conducted in Türkiye, the *Chryseobacterium* sp. strain C-204—responsible for mortalities in trout fry—was characterized and reported as an opportunistic pathogen (Saticioglu *et al*. 2019).

As with many pathogenic bacteria, antibiotic use is the most commonly preferred approach to control *Chryseobacterium* sp. In treating diseases caused by *Chryseobacterium* species, oxytetracycline, florfenicol, enrofloxacin, and, more rarely, antibiotics with amoxicillin or sulfamethoxazole–trimethoprim as active ingredients are typically employed (Loch and Faisal 2014). However, in recent years, antibiotic applications have become one of the most debated issues (Mohammed *et al*. 2025). Today, resistance mechanisms arising from the indiscriminate use of antibiotics constitute a major unresolved challenge. One of the major challenges in the management of *Chryseobacterium*-associated infections is the increasing prevalence of antimicrobial resistance, which substantially limits effective treatment options (Saticioglu *et al*. 2021). Comprehensive investigations have clearly demonstrated that these bacteria can develop resistance to broad-spectrum antibiotics, including β-lactams, aminoglycosides, and tetracyclines (Michel *et al*. 2005). Accordingly, there is a clear need for new, environmentally friendly, and cost-effective methods to control disease. In this regard, phage therapy has emerged as a promising alternative.

In recent years, bacteriophages (phages) have attracted attention as an innovative biocontrol strategy for managing bacterial infections. Phages are viruses that infect only the host bacterium and eliminate it through lysis (Nhung *et al*. 2025). Naturally present in aquatic ecosystems, phages can act against pathogens with high specificity, thereby sparing beneficial microbiota (Üstündağ 2025). Moreover, using phages as therapeutic agents holds great potential for curbing the spread of antibiotic resistance. To date, there are no phage studies specifically targeting diseases caused by *Chryseobacterium* sp. in aquaculture. It is evident that further phage research on *Chryseobacterium* sp. is needed for effective disease control.

This study aims to develop an effective bacteriophage against *Chryseobacterium* sp., a pathogen that causes serious economic losses in trout production—an important species in both global and national aquaculture—and that has developed resistance to antibiotics. In this context, this is the first isolation and characterization of *Chryseobacterium* sp. phages, its antibiotic resistance mechanisms, and the potential role of phages in aquaculture will be examined in detail. The study is expected to contribute to the development of alternative approaches in aquatic animal disease management and to environmental sustainability.

## 2 | METHODOLOGY

### 2.1 Isolation of bacteria

In this study, for the isolation of *Chryseobacterium* sp., samples were collected from newly dead diseased fish in trout farms located in Mersin and Van (Türkiye) between May and October 2024. The fish were transported to the laboratory under a cold chain, and inoculations from the liver, spleen, kidney, and gills of fry were performed onto Anacker–Ordal medium under aseptic conditions. The inoculated plates were incubated at 20 – 25°C for 3 – 5 days. At the end of incubation, yellow-pigmented colonies resembling *Chryseobacterium* sp. were observed on the medium. Individual colonies were subcultured repeatedly until a single colony was obtained, and pure cultures were established (Li *et al*. 2025).

### 2.2 Identification of bacteria

For identification of *Chryseobacterium* sp., rapid diagnostic kits (API 20E and API ZYM, bioMérieux) were used to determine biochemical characteristics, and bacterial identification was confirmed by 16S rRNA analysis (Oosthuizen 2018). For phenotypic characterization, Gram staining, cytochrome oxidase, catalase, motility by hanging drop, starch hydrolysis, gelatin hydrolysis, oxidation–fermentation (O/F) test, and detection of flexirubin pigment were performed. In addition, API ZYM and API 20E test kits were used to determine the biochemical profile of the strain (see Tables S1 – S3). Isolated colonies were incubated on Anacker–Ordal medium for 24 h. For species determination, DNA was extracted from the isolates using the GeneMATRIX kit (EurX, Poland) according to the manufacturer's instructions. DNA quantity and purity were assessed with a NanoDrop 2000 spectrophotometer (Thermo Scientific, USA). Universal primers 27F–1492R were used for PCR amplification, carried out with FIREPol® DNA polymerase (Solis Biodyne, Estonia). The ther-

mal cycling protocol consisted of an initial denaturation at 95°C for 5 min; 40 cycles of 95°C for 45 s, 57°C for 45 s, and 72°C for 60 s; followed by a final extension at 72°C for 5 min. Amplicons were analyzed by electrophoresis on 1.5% agarose gels (1 × TAE buffer) and visualized under UV. Single-band products were purified using the HighPrep™ PCR Clean-up System (MAGBIO, AC-60005). Sanger sequencing was performed at Macrogen (The Netherlands) using an ABI 3730XL instrument and the BigDye Terminator v3.1 Cycle Sequencing Kit (Applied Biosystems, USA). Forward (27F) and reverse (1492R) reads were assembled into contigs to generate consensus sequences (Stenholm *et al*. 2008).

**2.3 Antibiotic susceptibility testing**

Antibiotic susceptibilities of the isolated and identified *Chryseobacterium* sp. strain were determined by the Kirby–Bauer disk diffusion method in accordance with the standards of the Clinical and Laboratory Standards Institute (CLSI) and the European Committee on Antimicrobial Susceptibility Testing (EUCAST) (CLSI 2014; EUCAST 2019). Disks (Oxoid, Basingstoke, UK) of antibiotics commonly used in trout were tested: sulfamethoxazole (25 µg), erythromycin (15 µg), enrofloxacin (5 µg), florfenicol (30 µg), oxolinic acid (2 µg), ampicillin (10 µg), neomycin (10 µg), trimethoprim (5 µg), oxytetracycline (30 µg), amoxicillin (10 µg), clindamycin (2 µg), rifampicin (5 µg), gentamicin (10 µg), amikacin (30 µg), tetracycline (30 µg), ciprofloxacin (10 µg), chloramphenicol (30 µg), piperacillin (100 µg), piperacillin–tazobactam (100/10 µg), cefotaxime (30 µg), ceftazidime (30 µg), cefepime (30 µg), aztreonam (30 µg), imipenem (10 µg), meropenem (10 µg), kanamycin (30 µg), streptomycin (10 µg), doxycycline (30 µg), minocycline (30 µg), norfloxacin (10 µg), ofloxacin (5 µg), and nalidixic acid (30 µg). The identified Chryseobacterium sp. strain was inoculated into Anacker–Ordal broth and incubated at 20 – 25°C for 3 – 5 days. A bacterial suspension adjusted to 0.5 McFarland (≈$1\times10^8$ CFU $mL^{-1}$) was prepared and 0.1 mL was spread evenly onto Mueller–Hinton agar (Sigma-Aldrich, UK; 3 g $L^{-1}$). Approximately 15 min after inoculation, antibiotic disks were placed using sterile forceps. Following incubation, inhibition zones were measured with callipers and interpreted according to CLSI/EUCAST criteria. Each assay was performed at least in triplicate, and results were calculated as the mean of replicates (EUCAST 2019).

**2.4 Isolation of bacteriophages and double-layer agar plaque method**

Water samples for phage isolation were collected from tanks containing newly dead diseased fish at trout farms in Mersin and Van, and were logged (Table S3). Each sample was transferred into 15 mL Falcon tubes and centrifuged at 10,000 × g for 10 min, then gently filtered through 0.22 µm membranes (Wang *et al*. 2017). For enrichment, each filtrate (1 mL) was mixed with 1 mL of *Chryseobacterium* sp. culture in Anacker–Ordal broth and incubated at a constant temperature of 20°C for 5 days. Temperature was strictly controlled using an incubator throughout the entire enrichment period to avoid fluctuations that could affect phage-host interaction kinetics. The selected temperature reflects the optimal growth conditions of *Chryseobacterium* sp. and is consistent with temperatures commonly used for the isolation of phages infecting members of the family Flavobacteriaceae. Following enrichment, chloroform (50 µL $mL^{-1}$) was added to the supernatant, which was subsequently clarified and re-filtered through 0.22 µm membranes (Sundell *et al*. 2020). The presence of phages in the supernatant was assessed using the double-layer agar method. Briefly, 100 µL of phage preparation was mixed with 300 µL of *Chryseobacterium* sp. culture in the exponential growth phase (18 – 24 h) and incubated at 20°C under constant temperature conditions for 30 min. The mixture was then combined with 4,000 µL of molten soft agar (top agar, 0.4%) maintained at 48 – 50°C and immediately poured onto previously prepared plates. Plates were incubated at 20°C for 3 – 5 days, after which plaque formation was recorded.

**2.5 Single-plaque isolation**

Phages exhibiting lytic activity were purified by single-plaque isolation. A total of 100 µL of phage preparation was mixed with 500 µL of *Chryseobacterium* sp. in the exponential phase (18 – 24 h) and incubated at 20 – 25°C for 30 min. After mixing with 4,000 µL of top agar (0.4%) at 48 – 50°C, the mixture was poured onto plates and incubated at 20 – 25°C for 3 – 5 days. A single, well-isolated plaque was picked with a sterile Pasteur pipette, transferred into SM buffer, and gently agitated for at least 2 h. Following chloroform extraction (32 µL $mL^{-1}$) and centrifugation (9,000 × g, 20 min), the filtrate was transferred to a sterile tube. This procedure was repeated at least three times. The host was reinfected and plaque purification was repeated to obtain a single phage clone (Stenholm *et al*. 2008).

**2.6 Determination of kinetic parameters of bacteriophages**

A total of 500 µL of phage preparation with a known initial titer ($10^7$ PFU $mL^{-1}$) was mixed with 1,000 µL of *Chryseobacterium* sp. in the exponential phase ($10^8$ CFU $mL^{-1}$), resulting in a multiplicity of infection (MOI) of approximately 0.05 and incubated at 20 – 25°C for 10 min. After centrifugation, the bacteria were resuspended in 1,000 µL of cold Anacker–Ordal broth and then combined with 60 mL of cold Anacker–Ordal broth. Aliquots were sampled every 30 min for 8 h and plated using the double-layer agar method, followed by incubation at 20 – 25°C (Stenholm *et al*. 2008). Plaques were counted and rec-

orded. All single-step growth experiments were performed in triplicate ($n$ = 3) as independent biological replicates. A plateau in phage titers indicated the latent period (Gümüştaş 2015). Burst size was calculated as the ratio of the maximum phage titer (PFU/mL) reached after the latent period to the phage titer measured during the latent period, according to the following equation:

Burst size = Maximum phage titer (PFU/mL) / Phage titer during the latent period (PFU/mL)

For adsorption assays, *Chryseobacterium* sp. cultures (30 mL, exponential phase) were mixed with phages at the same initial MOI and incubated at 20 – 25°C. Samples were taken every 5 min for 30 min, diluted 1:10 in SM buffer containing chloroform (50 µL $mL^{-1}$), mixed thoroughly, and centrifuged (5,000 × g, 3 min). Supernatants were promptly plated by the double-layer method and incubated at 20 – 25°C; plaques were then enumerated (Castillo *et al*. 2022). Each adsorption experiment was conducted in triplicate. The percentage adsorption was calculated from the titer of unabsorbed phages in the supernatant as:

%adsorption = (Initial titer – Post-adsorption titer) / Latent-period titer × 100.

The adsorption constant ($K$) was computed as:

$K = (2.3 / B\ t)\ \log x\ (P_0 / P)$

where $K$ is the adsorption constant, $B$ is the bacterial concentration (cells $mL^{-1}$), $t$ is time, $P_0$ is the PFU at time zero, and $P$ is the PFU remaining in the supernatant. All kinetic parameters are presented as mean ± standard deviation (SD) calculated from three independent experiments.

**2.7 Determination of phage host range**

To determine whether the purified phages were specific to *Chryseobacterium* sp., spot tests were performed against nine *Chryseobacterium* sp. isolates obtained in this study and the following bacterial strains: *Flavobacterium psychrophilum*, *Chryseobacterium* sp., *Chryseobacterium chaponense*, *Chryseobacterium* spp., *Enterococcus casseliflavus*, *Salmonella* Typhimurium, *Staphylococcus aureus*, *Pseudomonas aeruginosa*, *Bacillus subtilis spizizenii*, *Enterobacter hormaechei*, *Escherichia coli*, *Enterococcus faecalis*, and *Pseudomonas putida*.

**2.8 Electron microscopy of bacteriophages**

Phage suspensions were mixed 1:10 with 2.5% glutaraldehyde buffer and incubated at room temperature for 5 min. The suspensions were then applied onto Formvar–carbon-coated copper grids and allowed to adsorb for 2 min at room temperature. Excess fluid was removed with filter paper. Phages were negatively stained with 2% uranyl acetate for 2 min at room temperature; excess stain was wicked off and specimens were rinsed with distilled water. Phages were subsequently visualized by TEM (Yıldızlı *et al*. 2022).

**2.9 Purification of bacteriophage DNA**

For DNA purification, phage filtrates were transferred to fresh microtubes. DNase and RNase were added to each tube and incubated at 37°C for 30 min, followed by PEG 8000 precipitation on ice for 1 h. Samples were centrifuged at 11000 rpm for 10 min at 4°C; the supernatant was discarded, and the pellet was resuspended in 500 µL of resuspension buffer and transferred to new tubes. For each 500 µL of phage suspension, 10 µL of 0.5 M EDTA and proteinase K to a final concentration of 100 µg $mL^{-1}$ were added. After incubation at 50°C for 30 min, genomic DNA was purified using the GeneJET Gel Extraction and Cleanup Micro Kit according to the manufacturer's protocol (Yıldızlı *et al*. 2022). Phage genome sizes were assessed by agarose gel electrophoresis. Phage DNA was digested with the restriction endonuclease HindIII at 37°C for 2 h, and the reaction was terminated by incubation in a water bath at 80°C for 20 min (Castillo *et al*. 2012). The genomic DNA was analyzed on 0.7% agarose gels prepared in Tris–boric acid–EDTA (TBE) buffer. For each bacterium, both HindIII-digested and undigested DNA were loaded. Electrophoresis was run at 70 V for 120 min (Castillo *et al*. 2012). The gel was then stained with ethidium bromide (EtBr, 1 µg $mL^{-1}$) for 10 min and visualized on a transilluminator. Chromosomal DNA sizes were estimated using GelPro (Yıldızlı *et al*. 2022).

**3 | RESULTS**

**3.1 Isolation of bacteria**

Samples taken from fish livers, gills, and skin were inoculated onto Anacker–Ordal medium and incubated at 20 – 25°C for 3 – 5 days. Yellow-pigmented colonies, morphologically resembling *Chryseobacterium* sp.—with a raised central area and finely spreading margins—were purified. To determine the biochemical characteristics of *Chryseobacterium* sp. isolates, rapid diagnostic kits (API 20E and API ZYM, bioMérieux) were used and the biochemical profiles were established (Table S4). In API 20E testing, LDC, ODC, and VP were positive. In contrast, IN was negative in *Chryseobacterium* sp. 3, URE was negative in *Chryseobacterium* sp. 4, and $H_2S$ was negative in *Chryseobacterium* sp. 6 and *Chryseobacterium* sp. 9. Additionally, unlike the other strains, CIT was negative in *Chryseobacterium* sp. 4 and *Chryseobacterium* sp. 6 (Table S1 – S2). Genomic DNA was extracted from the strains. The 16S rRNA gene region was amplified by PCR, and sequence analysis was matched to reference genomes in the NCBI GenBank. The similarity was 98.93%. Accession for *Chryseobacterium* sp. 1: GenBank PP462175 (sequence ID: Seq1; release date: 04/08/2026 double check).

**3.2 Antibiotic susceptibility testing**

Antibiotic susceptibility/resistance was examined using the Kirby–Bauer disk diffusion method. Based on inhibi-

tion zone diameters, susceptibility levels were interpreted according to CLSI and EUCAST standards. According to these criteria, *Chryseobacterium* sp. strains were susceptible to enrofloxacin (ENR, 5 µg), oxolinic acid (OA, 2 µg), ciprofloxacin (10 µg), norfloxacin (NOR, 10 µg), and ofloxacin (OFX, 5 µg); moderately susceptible to oxytetracycline (OT, 30 µg) and minocycline (MIN, 30 µg); and resistant to all other antibiotics listed in Table S3.

**3.3 Single-plaque isolation of bacteriophages and double-layer agar plaque method**

Water from which the bacteria had been isolated was used for phage isolation. Following centrifugation, filtration, and chloroform treatment as described, the presence of phages was confirmed by the double-layer agar method. Nineteen lytic phages were obtained and designated CV1–CV19.

**3.4 Kinetic parameters of bacteriophages**

The latent period of CV5 was approximately 2.5 h, whereas CV12 and CV9 exhibited latent periods of 8 h. The remaining phages had latent periods between 2, 5 and 8 h. The highest burst size was observed for CV5 (Table 1). Growth curves showed near-linear trends across phages (Figure 1). Burst size values ranged between 2.55 ± 22.52 and 235 ± 100 phage/cell across all isolates. The highest value was recorded for CV5 (235 ± 100 phage/cell). This was followed by CV16 (29.25 ± 31.41), CV18 (25 ± 17), CV7 (24.25 ± 29.75), CV6 (23.5 ± 29), CV4 (22.5 ± 29.16), and CV3 (22 ± 29). Isolates showing moderate burst size included CV1 (46.75 ± 37.25) and CV2 (19.25 ± 28.09). The lowest burst size values were observed in isolates CV8 – CV15, where most values clustered between 2.55 and 2.93 phage/cell.

**3.5 Phage adsorption**

Adsorption data indicated that all phages began binding to the bacterial surface from 0 min onward (Figure 2). All 19 phages (CV1 – CV19) showed attachment by the 5$^{th}$ min, with marked increases after 25 min. Notably, CV6 and CV7 exhibited increased attachment from 20 min. By 30 min, CV19 reached 100% adsorption, whereas CV13 showed comparatively lower attachment. Adsorption kinetics further revealed time-dependent variations in binding efficiency among the phage isolates. In CV1, CV3, and CV10, a pronounced increase in attachment was observed after the 10$^{th}$ minute, whereas CV12 and CV14 exhibited a more gradual adsorption trend. Notably, a rapid acceleration in binding was recorded for CV5, CV16, and CV18 between 20 and 25 min, approaching optimal adsorption levels. Overall, most isolates achieved high adsorption capacity before reaching the 30$^{th}$ minute; however, a clear heterogeneity in attachment efficiency was evident across the phage population.

**3.6 Determination of phage host range**

Host range was assessed for the 19 phages against the nine *Chryseobacterium* sp. isolates and other species (Figure S1). In our study, host range was evaluated in two parts: (i) spot tests on the isolated *Chryseobacterium* sp. 1–9 strains, and (ii) tests on other bacterial species known not to be the primary hosts. In the first part, the phages inhibited nearly all *Chryseobacterium* sp. host strains.

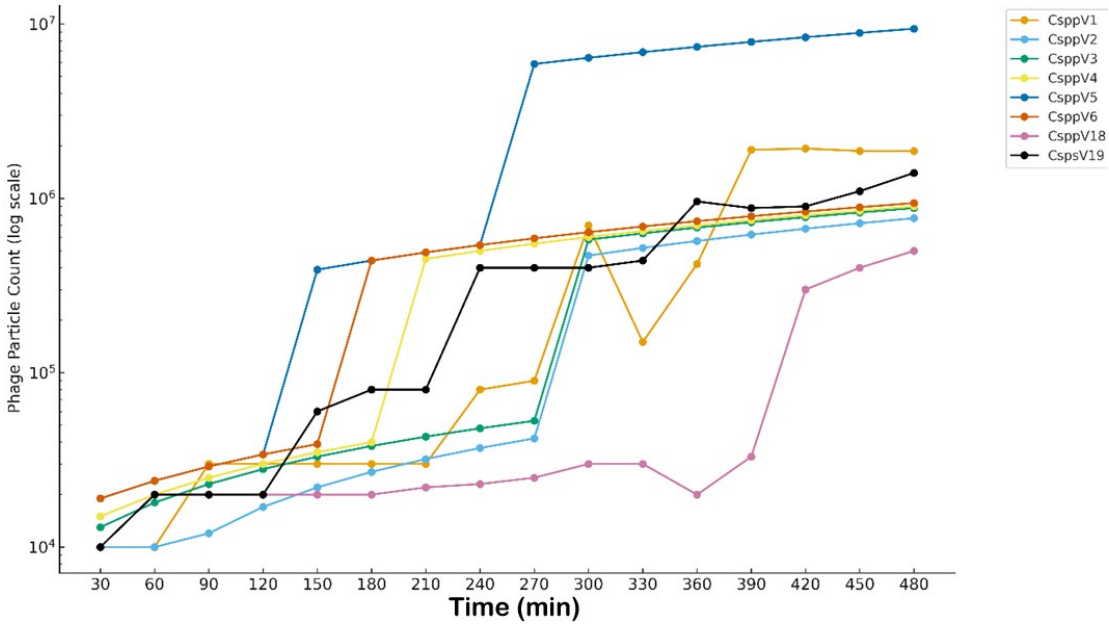


**FIGURE 1** Latent period and burst size.

**TABLE 1** Latent period, burst size, genome size, and adsorption constant (K) of isolated phages.

| Faj | Genome size (kb) | Latent period (hour) | Burst size (phage/cell) | Phages adsorption constant (K) |
|---|---|---|---|---|
| CV1 | 52 | 5 | 46,75±37,25 | $1.38 \times 10^{-6} \pm 1.27 \times 10^{-6}$ |
| CV2 | 55 | 5 | 19,25±28,09 | $1.86 \times 10^{-6} \pm 1.79 \times 10^{-6}$ |
| CV3 | 55 | 5 | 22±29 | $2.55 \times 10^{-6} \pm 1.69 \times 10^{-6}$ |
| CV4 | 55 | 3.5 | 22,5±29,16 | $2.43 \times 10^{-6} \pm 1.68 \times 10^{-6}$ |
| CV5 | 52 | 2.5 | 235±100 | $2.07 \times 10^{-6} \pm 1.83 \times 10^{-6}$ |
| CV6 | 52 | 3 | 23,5±29, | $1.86 \times 10^{-6} \pm 2.77 \times 10^{-6}$ |
| CV7 | 52 | 3 | 24,25±29,75 | $2.07 \times 10^{-6} \pm 1.73 \times 10^{-6}$ |
| CV8 | 55 | 5 | 2,55±22,52 | $1.05 \times 10^{-6} \pm 1.32 \times 10^{-6}$ |
| CV9 | 48 | 8 | 2,55±22,52 | $1.86 \times 10^{-6} \pm 1.76 \times 10^{-6}$ |
| CV10 | 53 | 6 | 2,62±22,54 | $1.65 \times 10^{-6} \pm 1.36 \times 10^{-6}$ |
| CV11 | 48 | 5.5 | 2,675±22,56 | $1.59 \times 10^{-6} \pm 1.34 \times 10^{-6}$ |
| CV12 | 65 | 7.5 | 2,725±22,58 | $1.86 \times 10^{-6} \pm 1.44 \times 10^{-6}$ |
| CV13 | 65 | 7.5 | 2,825±22,6 | $1.49 \times 10^{-6} \pm 2.33 \times 10^{-6}$ |
| CV14 | 72 | 7 | 2,8±22,6 | $1.86 \times 10^{-6} \pm 1.76 \times 10^{-6}$ |
| CV15 | 72 | 7 | 2,925±22,64 | $2.07 \times 10^{-6} \pm 1.50 \times 10^{-6}$ |
| CV16 | 72 | 6.5 | 29,25±31,41 | $2.28 \times 10^{-6} \pm 1.61 \times 10^{-6}$ |
| CV17 | 75 | 6.5 | 2,9±22,63 | $1.65 \times 10^{-6} \pm 2.03 \times 10^{-6}$ |
| CV18 | 72 | 7 | 25±17 | $1.59 \times 10^{-6} \pm 1.41 \times 10^{-6}$ |
| CV19 | 65 | 7.5 | 2,9±25,9 | $1.89 \times 10^{-6} \pm 4,01 \times 10^{-6}$ |

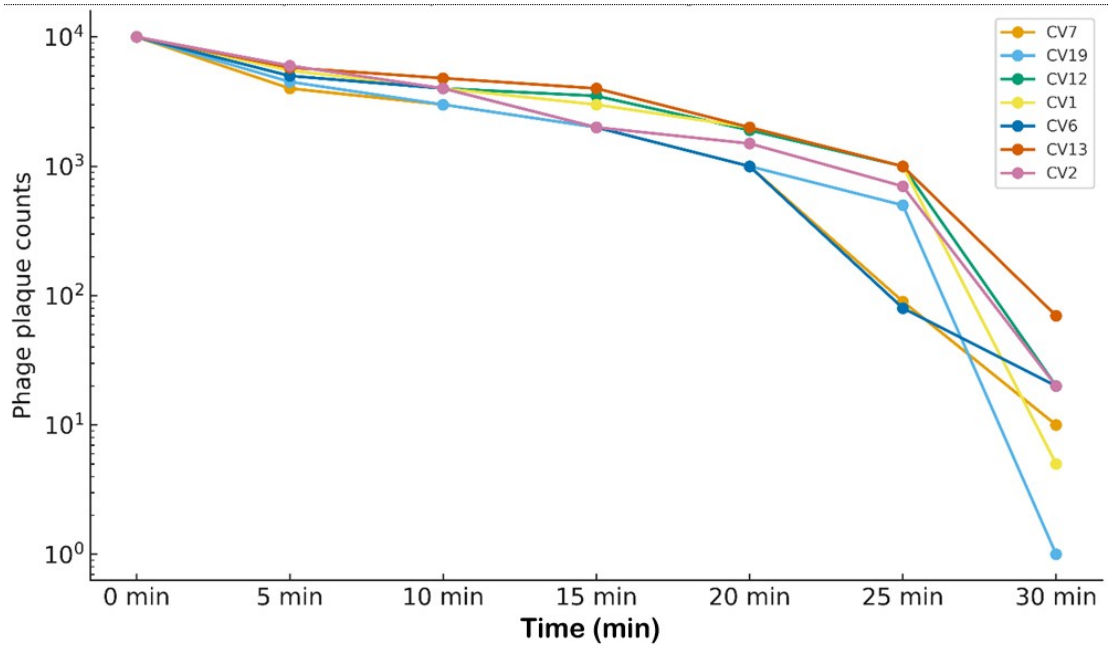


**FIGURE 2** Phage adsorption.

However, CV7 did not form plaques on *Chryseobacterium* sp.6; CV11 did not form plaques on *Chryseobacterium* sp. 3; CV14 did not form plaques on *Chryseobacterium* sp. 8; and CV16 did not form plaques on *Chryseobacterium* sp. 7. Additionally, turbid plaques were observed as follows: CV4 on *Chryseobacterium* sp. 8; CV7 on *Chryseobacterium* sp. 4; CV9 on *Chryseobacterium* sp. 4 and *Chryseobacterium* sp. 8; CV10 on *Chryseobacterium* sp. 2 and *Chryseobacterium* sp.; CV12 on *Chryseobacterium* sp. 8; CV13 on *Chryseobacterium* sp. 3; CV15 on *Chryseobacterium* sp. 8; and CV16 on *Chryseobacterium* sp. 5. In the second part, CV3 and CV16 produced clear plaques on the pathogen *F. psychrophilum*, while CV3, CV4, and CV18 produced turbid plaques on *E. faecalis*.

**3.7 Transmission electron microscopy of bacteriophages**

Prepared phage suspensions were negatively stained with uranyl acetate and processed for TEM visualization (Figure S2). TEM analysis of representative isolates CV1, CV2, CV7, and CV15 revealed well-defined viral particles with

distinct structural integrity, allowing clear visualization of capsid morphology and tail architecture. The observed phages exhibited uniform structural features, suggesting morphological consistency among the selected isolates. These findings confirm successful phage preparation and validate the reliability of TEM-based structural assessment for taxonomic and morphological classification.

### 3.8 Determination of genome size

Genome size analysis revealed that the phage isolates exhibited genomic lengths ranging from 48 kb to 75 kb (Figure 3). The smallest genomes were observed in CV9 and CV11 (48 kb), while the largest genome size was recorded for CV17 (75 kb). A cluster of isolates, including CV1, CV5, CV6, and CV7, displayed genome sizes of 52 kb, whereas CV2, CV3, CV4, and CV8 shared a similar size of 55 kb. Moderately larger genomes were identified in CV10 (53 kb) and CV12, CV13, and CV19 (65 kb). Isolates CV14, CV15, CV16, and CV18 exhibited genome sizes of 72 kb, representing the second highest size group. Overall, the data demonstrate a heterogeneous genomic distribution, with isolates forming distinct size groups that reflect variability in their genomic architecture.

## 4 | DISCUSSION

In this study, the role of *Chryseobacterium* sp. as an important pathogen in aquaculture was examined, and data were generated toward phage-based control strategies against this bacterium. Because no prior studies exist for the isolated taxon, comparisons are made with previously described *Chryseobacterium* species.

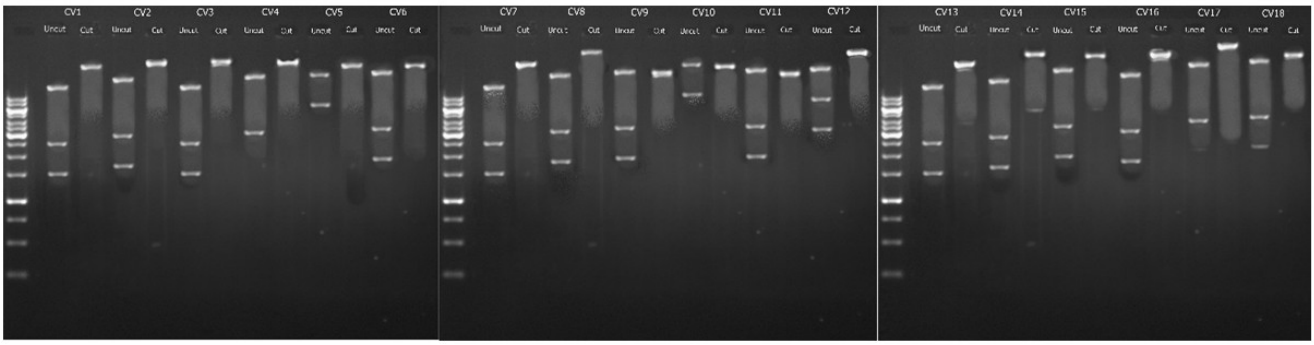


**FIGURE 3** Genome sizes of *Chryseobacterium* sp. phages.

We conducted a detailed analysis of kinetic parameters for 19 phages isolated from nine *Chryseobacterium* strains, determining single-step growth metrics including latent period, burst size, and adsorption rate constant. Overall, the values align with those reported for other aquatic phages. Some *Chryseobacterium* phages have short latent periods of ~20 – 30 min–comparable to phages of similar Gram-negative aquatic pathogens. Indeed, for the phage MA9V-1 infecting *Chryseobacterium indologenes*, the latent period is ~20 min (Zou *et al*. 2023). Nonetheless, latent times can vary markedly with temperature and host growth rate, ranging from ~10 min to 2 h in aquatic systems (Fister *et al*. 2016). Burst sizes among our phages also varied: some produced ~10 – 20 progeny per cell, whereas others reached 50 – 100. While MA9V-1 exhibits a relatively low burst size (~10 PFU cell$^{-1}$) (Zou *et al*. 2023), certain broader-host-range phages infecting Vibrio spp. may exceed 300 (Fister *et al*. 2016), reflecting differences in genomic architecture and life-history strategies. With respect to adsorption, most of our 19 phages bound rapidly to host cells; similarly, many aquatic phages adsorb to >50% of cells within 5 – 10 min MA9V-1 reaches ~75% binding within 8 min (Zou *et al*. 2023). Overall, our phages exhibit short latent periods (<1 h), moderate burst sizes, rapid adsorption, comparable to other Flavobacteriaceae phages.

Host-range analyses for our 19 phages encompassed both intraspecific (multiple strains of the same species) and interspecific (different species) levels. The general trend indicates narrow host ranges: individual phages typically infect only the isolation host or very closely related strains. This high specificity is widely reported for lytic phages (Donati *et al*. 2021). For example, MA9V-1 infects only *C. indologenes* strains and does not form plaques on Gram-positive bacteria or other Gram-negative genera (e.g. *Bacillus, Pseudomonas,* and *Escherichia coli*) (Zou *et al*. 2023). Intraspecifically, some phages can lyse several strains of the same *Chryseobacterium* species, whereas others lyse only one or two. Analogously, among phages of *F. psychrophilum*, some infect 5/28 strains while others infect up to 23/28, each phage exhibiting a unique host pattern. This underscores specialization even within a single bacterial species. Interspecifically, most of our phages formed plaques only on their primary *Chryseobacterium* hosts or closely related strains; a few exceptions infected more than one *Chryseobacterium* species. None infected distant genera; host range did not extend beyond Flavobacteriaceae. Although rare "polyvalent" phages can cross family boundaries, such breadth is exceptional and was not observed here. The high specificity reflected by our isolates is therefore consistent with canonical phage–host interactions.

Molecularly, phage infection resembles a key–lock fit: tail fibers or spike proteins recognize specific receptors (e.g. O antigens, porins, flagella, and pili) on the bacterial surface. Thus, each phage infects bacteria compatible with its receptor-binding protein (RBP) repertoire. Although comprehensive genomics of our 19 phages is pending, *Chryseobacterium* phages are frequently tailed phages within *Caudoviricetes*, bearing specialized RBPs. MA9V-1, for example, displays a hemicosahedral head (~121 nm) and a contractile tail (~170 nm), consistent with a myovirus-like morphology (Zou *et al*. 2023). Its narrow host range implies RBPs targeting a specific *C. indologenes* surface determinant (e.g. an LPS epitope or outer-membrane protein). A second determinant is host defense. Even after DNA injection, restriction–modification systems or CRISPR–Cas can degrade phage genomes. In the natural "arms race" between *Flavobacterium columnare* and its phages, CRISPR spacers accumulate in the bacterium while phages accrue mutations in protospacers to evade recognition (Laanto *et al*. 2017). Phages may evolve anti-CRISPR proteins or DNA modifications to resist restriction. These mechanisms co-define host specificity. In our context, phages infecting multiple *Chryseobacterium* species likely target a receptor shared among those species; highly strain-specific phages probably recognize unique, strain-level structures. Future genomic analyses (e.g. tail fiber/RBP gene diversity) will clarify these molecular bases of specificity. For now, the literature supports that RBPs and host defense systems jointly shape phage host range (Laanto *et al*. 2017).

The genus *Chryseobacterium* encompasses opportunistic pathogens of environmental, clinical, and aquaculture relevance. Some species (e.g. *C. scophthalmum* and *C. balustinum*) cause fish infections and economic losses (Mallik *et al*. 2023), whereas others (e.g. *C. indologenes* and *C. gleum*) can lead to difficult-to-treat human infections (Izaguirre-Anariba and Sivapalan 2020). Against *Chryseobacterium*-associated infections, bacteriophages offer an alternative therapeutic approach, regaining attention amidst escalating antibiotic resistance (Donati *et al*. 2021). *Chryseobacterium* strains often harbor multidrug-resistance determinants (e.g. β-lactamases). Phages, by contrast, can selectively kill the pathogen while sparing commensal microbiota. Encouraging outcomes have been reported against aquatic pathogens in *Flavobacterium* and *Chryseobacterium*. For instance, phage FCL-2 reduced mortality from columnaris disease caused by *F. columnare* and lowered pathogen load in water (Laanto *et al*. 2015). Likewise, the MA9V-1 phage targeting the plant pathogen *C. indologenes* MA9 mitigated disease in vivo when applied to infected roots (Zou *et al*. 2023) demonstrating broader translational potential beyond animals. Phage cocktails are a key strategy to overcome narrow host ranges: combining phages that target different strains expands coverage and slows resistance evolution (Donati *et al*. 2021). Our panel of 19 phages provides a candidate pool for such cocktails—for example, pairing phages active against *C. balustinum*-like strains with those targeting *C. indologenes*-like strains to jointly suppress both groups. Safety and stability are critical for application. Absence of integrases, toxins, and antibiotic-resistance genes in phage genomes would support their suitability as therapeutic lytic phages (Zou *et al*. 2023). Environmental stability (temperature, pH) and production/administration logistics also matter: many aquatic phages remain stable between ~4 – 30°C and across broad pH ranges; some Vibrio phages tolerate up to 45°C and pH 5 – 8 (Fister *et al*. 2016). Similar assessments are needed for our *Chryseobacterium* phages to evaluate field applicability in aquaculture.

In summary, each of the 19 phages isolated here represents a candidate biocontrol agent against *Chryseobacterium*-driven infections under appropriate conditions. Contemporary literature increasing success stories in phage therapy and emphasizes that high host specificity enables elimination of target pathogens with minimal ecological perturbation (Fiedler *et al*. 2023).

An inevitable consideration in both applied and natural phage use is bacterial resistance and its ecological consequences. Bacteria frequently evade phages through mutations in surface receptors that block adsorption, leading to rapid selection of resistant variants. In *F. columnare*, phage-resistant mutants show altered surface structures and reduced virulence in fish, suggesting a fitness cost associated with resistance (Kunttu *et al*. 2021). However, not all resistance mechanisms impose such costs; CRISPR–Cas systems, for example, can eliminate phage DNA without apparent metabolic burden. Additional defense strategies include restriction–modification systems and abortive infection (Abi), where infected cells undergo altruistic death to prevent phage spread, reflecting an ongoing coevolutionary arms race (Laanto *et al*. 2017). In therapeutic contexts, phage cocktails and sequential phage application are recommended to delay resistance development (Donati *et al*. 2021). Using multiple phages reduces resistance risk but requires ongoing monitoring and rotation.

Phages regulate bacterial communities through "kill-the-winner" dynamics and contribute to nutrient cycling via the "viral shunt" (Wommack and Colwell 2000). In aquaculture, they can naturally reduce pathogen loads, and supplemental phage application is useful when endogenous pressure is low. Owing to their narrow host range, phage treatments typically cause minimal microbiota disruption (Fiedler *et al*. 2023); for example, targeting *F. columnare* reduced only the pathogen (Fiedler *et al*. 2023). Although transduction is a potential ecological concern, strictly lytic phages pose low risk when genomes lack harmful genes.

## 5 | CONCLUSIONS

This study provides an integrated characterization of aquatic *Chryseobacterium isolates*, revealing overall taxonomic consistency but notable variation in biochemical traits, substrate utilization, and antibiotic sensitivity, likely shaped by micro-habitat conditions and phage pressure. The nineteen isolated phages showed rapid adsorption, short latent periods, moderate burst sizes, and mainly narrow host ranges, indicating efficient and highly specific lytic activity suitable for targeted phage therapy and ecological control in aquaculture.

Future applications include developing strain-tailored phage cocktails as sustainable alternatives to antibiotics. Advancing this approach will require combining phenotypic data with genomic and proteomic analyses to clarify determinants of host range, resistance, and environmental stability, supported by comparative genomics, metagenomics, in vivo trials, and long-term monitoring. Overall, the findings underscore the strong potential of phage-based strategies for sustainable pathogen control and reduced antimicrobial use in aquaculture.

## ACKNOWLEDGEMENTS

The author would like to thank Van Yüzüncü Yıl University Scientific Research Projects Unit for financial support under Project No. FYD-2023-10871.

## CONFLICT OF INTEREST

The authors declare that they have no conflict of interest.

## AUTHORS' CONTRIBUTION

Both authors contributed equally to all stages of the study, including conceptualization, experimental design, data collection, data analysis, interpretation of results, and preparation of the manuscript. Both authors have read and approved the final version of the manuscript.

## DATA AVAILABILITY STATEMENT

All data generated or analyzed during this study are available from the corresponding author upon reasonable request.

## REFERENCES

Castillo D, Higuera G, Villa M, Middelboe M, Dalsgaard I, … Espejo RT (2012) Diversity of *Flavobacterium psychrophilum* and the potential use of its phages for protection against bacterial cold-water disease in salmonids. Journal of Fish Diseases 35(3): 193–201.

Castillo D, Højsting AR, Roosvall A, Smyrlis G, Jørgensen J, Middelboe M (2022) In vitro evolution of specific phages infecting the fish pathogen *Flavobacterium psychrophilum*. Phage 3(1): 28–37.

Clinical and Laboratory Standards Institute (CLSI) (2014) Performance standards for antimicrobial susceptibility testing of bacteria isolated from aquatic animals. CLSI document VET03/04-S2, Wayne, PA.

De Schryver P, Defoirdt T, Boon N, Verstraete W, Bossier P (2012) Managing the microbiota in aquaculture systems for disease prevention and control. In: Handbook of microalgal culture. Woodhead Cambridge, UK.

Donati VL, Dalsgaard I, Sundell K, Castillo D, Er-Rafik M, … Madsen L (2021) Phage-mediated control of *Flavobacterium psychrophilum* in aquaculture: in vivo experiments to compare delivery methods. Frontiers in Microbiology 543: 736946.

European Committee on Antimicrobial Susceptibility Testing (EUCAST) (2019) Zone diameter breakpoints for rapid antimicrobial susceptibility testing. Version 1.1.

Fiedler AW, Gundersen MS, Vo TP, Almaas E, Vadstein O, Bakke I (2023) Phage therapy minimally affects the water microbiota in an Atlantic salmon (*Salmo salar*) rearing system while still preventing infection. Scientific Reports 13: 19145.

Fister S, Robben C, Witte AK, Schoder D, Wagner M, Rossmanith P (2016) Influence of environmental factors on phage–bacteria interaction. Frontiers in Microbiology 7: 1152.

Gümüştaş A (2015) Laktik Asit Bakterileri ve Bakteriyofajlarının Çeşitli Kaynaklardan İzolasyonu ve Karakterizasyonu. Yüksek Lisans Tezi, Ankara Üniversitesi (in Turkish).

Huang C (2025) Clinical and Epidemiological features and antimicrobial susceptibility patterns of *Chryseobacterium* species: a scoping review. Medicina 61(7): 1197.

Izaguirre-Anariba DE, Sivapalan V (2020) *Chryseobacterium indologenes*, an emerging bacteria: a case report and review of literature. Cureus 12(2): e7000.

Kämpfer P, Busse HJ, McInroy JA, Glaeser SP (2015) *Chryseobacterium sediminis* sp. nov., isolated from a river sediment. International Journal Systematic and Evolutionary Microbiology 65: 3147–3153.

Kunttu HMT, Runtuvuori-Salmela A, Sundell K, Wiklund T, Middelboe M, … Sundberg LR (2021) Bacteriophage resistance affects *Flavobacterium columnare* virulence partly via mutations in genes related to gliding motility and the type IX secretion system. Applied and Environmental Microbiology 87: e00812-21.

Laanto E, Bamford JKH, Ravantti JJ, Sundberg LR (2015) The use of phage FCL-2 as an alternative to chemotherapy against columnaris disease in aquaculture. Frontiers in Microbiology 6: 829.

Laanto E, Hoikkala V, Ravantti J, Sundberg LR (2017) Long-term genomic coevolution of host–parasite interaction in natural environments. Nature Communications 8: 111.

Li M, Cai Y, Tian Y, Ke X, Zhao Z, … Wang S (2025) First isolation of *Chryseobacterium* sp. as a pathogen of fish eggs. Aquaculture Reports 43: 102992.

Loch TP, Faisal M (2014) *Chryseobacterium aahli* sp. nov., isolated from lake trout (*Salvelinus namaycush*) and brown trout (*Salmo trutta*), and emended descriptions of *Chryseobacterium ginsenosidimutans* and *Chryseobacterium gregarium*. International Journal of Systematic and Evolutionary Microbiology 64: 2985–2993.

Mallik SK, Pathak R, Shahi N, Kala K, Chandra S, … Pandey PK (2023) Pathological analysis and antimicrobial susceptibility of *Chryseobacterium balustinum* RTFCP 298 isolated from diseased rainbow trout, *Oncorhynchus mykiss*. Scientific Reports 13, 13268.

Michel C, Matte-Tailliez O, Kerouault B, Bernardet JF (2005) Resistance pattern and assessment of phenicol agents' minimum inhibitory concentration in multidrug resistant *Chryseobacterium* isolates from fish and aquatic habitats. Journal of Applied Microbiology 99: 1210–1216.

Mohammed EAH, Kovács B, Kuunya R, Mustafa EOA, Abbo ASH, Pál K (2025) Antibiotic resistance in aquaculture: challenges, trends analysis, and alternative approaches. Antibiotics 14(6): 598.

Nhung TTT, Verma S, Ponne S, Meghwanshi GK, Schön T, Kumar R (2025) Bacteriophage-based strategies for biocontrol and treatment of infectious diseases. Computational and Structural Biotechnology Journal 27: 2924-2932.

Oosthuizen L (2018) Taxonomy, growth and food spoilage characteristics of a novel *Chryseobacterium* species. MSc Thesis, Department of Microbial, Biochemical and Food Biotechnology, Faculty of Natural and Agricultural Sciences, University of the Free State, South Africa.

Rosado D, Xavier R, Severino R, Tavares F, Cable J, Pérez-Losada M (2019) Effects of disease, antibiotic treatment and recovery trajectory on the microbiome of farmed seabass (*Dicentrarchus labrax*). Sci Rep 9: Article 55314.

Saticioglu I B, Duman M, Altun S (2021) Genome analysis and antimicrobial resistance characteristics of *Chryseobacterium aquaticum* isolated from farmed salmonids. Aquaculture 535: 736364.

Saticioglu IB, Duman M, Smith P, Wiklund T, Altun S (2019) Antimicrobial resistance and resistance genes in *Flavobacterium psychrophilum* isolates from Turkey. Aquaculture 512: 734293.

Stenholm AR, Dalsgaard I, Middelboe M (2008) Isolation and characterization of bacteriophages infecting *Flavobacterium psychrophilum*. Applied and Environmental Microbiology 74(13): 4070–4078.

Stephen J, Mukherjee S, Lekshmi M, Kumar S (2023) Diseases and antimicrobial use in aquaculture. In: Mothadaka MP, Vaiyapuri M, Rao Badireddy M, Nagarajrao Ravishankar C, Bhatia R, Jena J (Eds) Handbook on Antimicrobial Resistance. Springer, Singapore

Sundell K, Landor L, Castillo D, Middelboe M, Wiklund T (2020) Bacteriophages as biocontrol agents for *Flavobacterium psychrophilum* biofilms and rainbow trout infections. Phage 1(4): 198–204.

Üstündağ M (2025) Phage therapy in aquaculture: applications, efficacy and challenges. MEMBA Water Sciences Journal 11(2): 182–200.

Wang C, Chuprom J, Wang Y, Fu L (2020) Beneficial bacteria for aquaculture: nutrition, bacteriostasis and immunoregulation. Journal of Applied Microbiology

Wang Y, Barton M, Elliott L, Li X, Abraham S, … Munro J (2017) Bacteriophage therapy for the control of *Vibrio harveyi* in greenlip abalone (*Haliotis laevigata*). Aquaculture 473: 251–258.

Wommack KE, Colwell RR (2000) Virioplankton: viruses in aquatic ecosystems. Microbiology and Molecular Biology Reviews 64(1): 69–114.

Yıldızlı G, Coral MNU, Coral G, Yılmaz SN (2022) Isolation and characterization of lytic bacteriophages infecting *Vibrio* sp. strains. Advances in Bioresearch 13(5): 1–10.

Zou H, Ding Y, Shang J, Ma C, Li J, … Wei Y (2023) Isolation, characterization and genomic analysis of a novel bacteriophage MA9V-1 infecting *Chryseobacterium indologenes*: a pathogen of *Panax notoginseng* root rot. Frontiers in Microbiology 14: 1251211.

***M Ustundag*** http://orcid.org/0000-0002-2990-4981
***B Ustundag*** http://orcid.org/0000-0001-5211-7874